LM-05K152
October 19, 2005

The Effect of Load-Line Displacement Rate on the SCC Growth Rate of Nickel Alloys and Mechanistic Implications

D Morton

THE EFFECT OF LOAD-LINE DISPLACEMENT RATE ON THE SCC GROWTH RATE OF NICKEL ALLOYS AND MECHANISTIC IMPLICATIONS

DS Morton
Lockheed Martin
Schenectady, NY 12301
P.O. Box 1072

ABSTRACT

A key set of SCC growth experiments was designed to test the hypothesis that deformation/creep is the rate controlling step in LPSCC. These tests were performed on Alloy X-750 AH compact tension specimens at a various constant displacement rates. The deformation/creep rate within the crack tip zone is proportional to the test displacement rate. If crack growth rates were observed to increase with the load–line displacement rate, then this would indicate that deformation/creep is a critical SCC mechanism process. However, results obtained from the load-line displacement tests did not find X-750 AH SCC growth rate to be dependent on the position rate and therefore do not support the assumption that deformation/creep is the rate controlling process in LPSCC. The similarities between the SCC response of X-750, Alloy 600 and EN82H suggests that it is likely that the same SCC process is occurring for all these alloys (i.e., the same rate controlling step) and that deformation based models are also inappropriate for Alloy 600 and EN82H. The strong temperature and coolant hydrogen dependencies exhibited by these alloys make it more likely that nickel alloy LPSCC is controlled by an environmental or corrosion driven process.

Keywords: stress corrosion cracking, SCC, crack tip strain rate, mechanisms, deformation

INTRODUCTION

The mechanism of nickel alloy low potential stress corrosion cracking (LPSCC) has been the subject of debate for several decades. Many of the mechanisms that have been postulated to describe LPSCC assume the rate of crack tip deformation as a critical mechanistic sub-process. For example, both the film rupture oxidation[1] (FRO) and Hydrogen Assisted Creep Fracture[2] (HACF) models assume that the SCC growth rate is directly proportional to crack tip strain rate ($\dot{\varepsilon}_{ct}$). Phenomenological based nickel alloy growth rate models have been

developed from both the FRO and HACF mechanisms[1, 2]. Mechanistic or phenomenological crack growth rate models are an improvement over empirically derived crack growth rate models[3] if the model is based on the correct mechanism/phenomena. That is, greater confidence would exist in extrapolations from mechanistic or phenomenological models compared to empirically based models. However, if the model is based upon an incorrect description of the SCC process then this model is not truly fundamentally based and in reality it is an empirical model. In this situation, if solid fundamental model supporting evidence does not exist then increased confidence should not be given to extrapolations from these models.

This document reports the results from load-line displacement rate SCC crack growth rate tests designed to quantify the dependency of nickel alloy crack growth rate upon the rate of crack tip deformation. The rate of deformation (i.e., creep) in the plastic zone of a growing SCC crack is proportional to $\dot{\varepsilon}_{ct}$ which in a load-line displacement test is proportional to the load-line displacement rate. Therefore, if increasing crack growth rates are observed, as the load-line displacement rate is increased in load-line displacement tests, then these results would be consistent with deformation based SCC models (e.g., HACF, FRO). However, if the crack growth rate does not vary with changes in the load-line displacement rate, then deformation or creep based models are fundamentally incorrect for the material tested.

EXPERIMENTAL PROCEDURE

The composition of the Alloy X-750 condition AH heat 38F3X material that was employed in this study is provided in Table 1. X-750 is a precipitation hardenable alloy that exhibits a significant variation in SCC susceptibility depending upon the specific thermal treatment[4]. The X-750 AH condition (Hot worked, aged at 885°C for 24 hours and aged at 704°C for 20 hours) which was tested in this study is particularly susceptible to SCC[4].

TABLE 1: COMPOSITION OF X-750 AH HEAT 38F3X (WT%)

(Hot worked, aged at 885°C for 24 hours and aged at 704°C for 20 hours).

Yield strength of 751 MPa (109 ksi)

Ni	*Cr*	*Fe*	*C*	*Mn*	*Si*	*Cu*	*Al*	*Ti*	*S*	*Co*
72.60	15.75	7.09	0.05	0.15	0.24	0.23	0.61	2.39	0.007	0.05

The alloy X-750 was fabricated into standard 10.2 mm thick compact tension (CT) specimens. All specimens were fabricated in a longitudinal-transverse (LT) orientation. Test specimens were air fatigue precracked, to a nominal a/W [(1)] of 0.5 using the fatigue precracking procedure from ASTM E399 Annex 2.

[(1)] a is the distance between the crack tip and the load line. W is the distance between the load line and the specimen end (surface in which an unrestrained crack would ultimately intersect).

Constant load/constant displacement rate SCCGR tests were conducted in active load servoelectric machines with digital control electronics monitored through a computerized data acquisition system. A description of the recirculating high flow rate autoclave system has previously been described[5].

SCC growth rate tests are often conducted with compact tension (CT) specimens that are loaded via active load test frames to a constant test load. In these constant load SCC tests, the CT specimen opens apart at the load-line as the crack advances. Consequentially the test frame actuator must move to maintain a constant load on the test specimen. In contrast, in SCC growth rate load-line displacement tests, the specimen load-line is pulled apart at a constant rate and the resulting load is a function of the load-line displacement rate and the crack growth rate. Figure 1 provides a sketch contrasting the loading modes in classical constant load and constant load-line displacement rate SCC growth rate (SCCGR) tests.

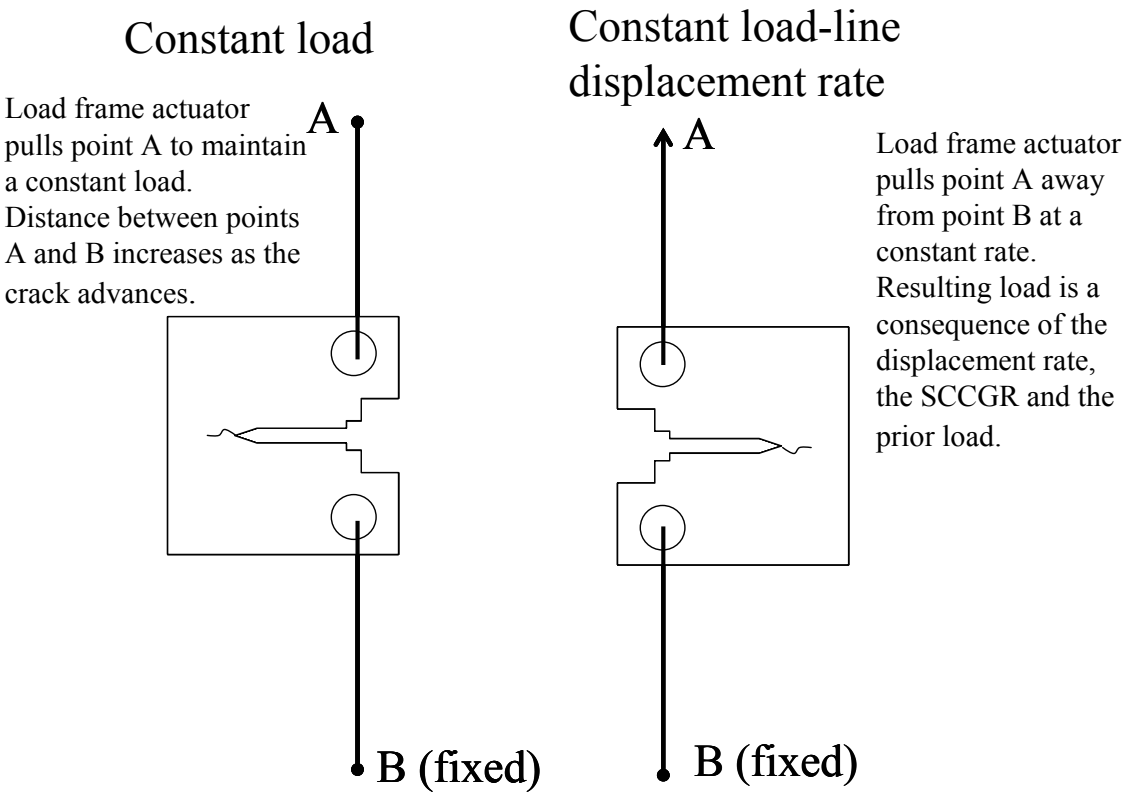

FIGURE 1: Sketch illustrating the loading modes in constant load and constant load-line displacement rate tests.

Test Environment

Tests were conducted at 316°C (600°F) with an autoclave pressure of 13.8 MPa (2000 psi) and 10 cc/kg dissolved hydrogen. The test chemistry was high purity deaerated water that was buffered to a room temperature pH of 10.1 to maintain a near neutral autoclave pH at the test temperature. Autoclave influent and effluent conductivities were continually measured through in-line conductivity probes. Trends in facility contaminant levels were additionally

monitored through system in-line conductivity probes. Absolute anion contaminant levels were verified as less-than-detectable by ion chromatography (IC) analysis of autoclave effluent samples. Autoclave cation contaminants were monitored through analysis of autoclave effluent samples by inductively coupled plasma spectroscopy (ICP) and were also less-than-detectable levels.

The 10 cc/kg hydrogen concentration was obtained by controlling the feed tank overpressure at 42 psig with a mixed gas of 15% hydrogen, with the balance being argon. A Henry's law coefficient of 0.85 psia/(cc/kg)[6] was used for these room temperature calculations. Since the autoclave turnover rate is relatively rapid (approximately every 30 minutes), autoclave effluent dissolved gas levels are analogous to feed tank levels. Oxygen levels for all tests were <10 ppb.

Test Load and Load-Line Displacements Rates

Three constant test conditions tests were conducted as part of this study, which consisted of 2 constant load-line displacement (position) rate tests and one constant load test. The two load-line displacement rate tests were conducted at actuator displacement rates of 0.00006 and 0.0003 in/hr (0.0015 and 0.0076 mm/hr). Each of these tests started at a stress intensity factor (K) of ~10 ksi√in (11 MPa√m) and were terminated at a K of ~68 ksi√in (75 MPa√m). The constant load test was conducted under pure constant load conditions to give a K of ~37 ksi√in (41 MPa√m).

In-situ Instrumentation

The onset and rate of SCC crack extension was monitored in-situ using reversing DC electrical potential drop (EPD) according to ASTM E647, Annex 3, and were verified by post-test destructive examinations (DE). EPD active voltages, which are proportional to crack extension, were normalized to account for material electrical resistivity changes that occur with time[7]. Load-line displacement was measured in-situ using front-face linear variable displacement transformers (LVDTs).

Electrochemical Corrosion Potential Measurements

Electrochemical corrosion potential (EcP) measurements were made during the tests by measuring the steady-state corrosion potential, or voltage, between the test specimen and a platinum reference electrode (e.g., a Pt wire or foil) and between the test specimen and an iron/iron oxide reference electrode. More information on EcP measurements during tests can be found in Reference (8).

Post-test Destructive Examinations (DEs)

Upon completion of the tests, specimens were heat-tinted at 450^{o}C in air for up to 12 hours to facilitate post-test crack measurements. Following heat-tinting, the specimens underwent an air fatigue extension of their cracks. This process avoids deformation of the SCC surface when the specimen is ultimately opened. The fatigue extended specimens were pulled-apart in tension to expose the fracture surfaces. The amount of SCC in each specimen was measured by optical examination using the procedure in ASTM E813. Average test crack

growth rates were determined by dividing the average SCC extension by the test duration in which crack growth occurred. The EPD indicated crack extension was corrected to match the actual DE determined crack length in an effort to provide the best possible representation of each test crack history. Additionally, scanning electron microscopy (SEM) inspections were performed on the fracture surfaces of the load-line displacement rate specimens to verify that the cracking morphology was intergranular.

RESULTS

Constant Load Test

Results from the X-750 AH constant load test are summarized in Figures 2-5 and in Table 2. Figure 2 illustrates that the test load was constant at 1287 ±1 lbs (583 kg) throughout the 13.2 day test. The EPD indicated crack history is provided in Figure 3. After a short incubation period of roughly 10 hours, a nearly constant crack growth rate was obtained. As noted in Figure 3, the actual test crack growth rate of 1.05 mils/day (1.11 μm/hr) was under predicted by the in-situ EPD crack monitor which showed 0.7 mils/day (0.7 μm/hr). Figure 4 illustrates that the stress intensity factor changed only slightly from 36.4 to 38.4 ksi√in (40.0 to 40.6 MPa√m) in this test indicating that a relatively constant K was maintained. The K values in Figure 4 were calculated from a DE corrected EPD crack history. In this constant load test, the 2.0 ksi√in (2.2 MPa√m) change in the K level is attributable directly to the 340 μm crack growth. This figure also indicates that the stress intensity factor increased linearly with time at 0.15 ksi√in/day (0.16 MPa√m/day). This constant rate of increase in K is a direct consequence of the linear crack extension history. Figure 5 gives the specimen load-line displacement response which was measured through an in-situ LVDT mounted to the specimen clevis. The LVDT displacement response appeared as a stepwise function with periodic jumps of ~8 mils. These jumps are not characteristic of the material SCC response (i.e., EPD did not show jumps) but are due to LVDT alignment problems. It is suspected that the LVDT barrel was dragging on the LVDT core such that a force, which was apparently equivalent to about 0.3 μm displacement, was needed to overcome the frictional force.

Constant Displacement Rate of 0.00006 in/hr (0.0015 mm/hr)

Results from the 0.00006 in/hr (0.0015 mm/hr) constant load-line displacement rate test are summarized in Figures 6-10 and in Table 2. Figure 6 provides the actuator position history which clearly shows that a constant displacement rate of 0.00006 in/hr was maintained throughout the 40.1 day test. Figure 7 illustrates that this constant displacement rate translated to a relatively constant rate of load increase (~53 lbs/day (24 kg/day)) throughout the test. The EPD indicated and DE corrected crack extension throughout the test is provided in Figure 8. An incubation period of ~ 40 hours was observed. Following this incubation period the crack growth rate increased slightly with time. The average SCCGR for this test was, however, only 0.64 mils/day (0.68 μm/hr). Recall that the average SCCGR was 1.05 mils/day (1.11 μm/hr) in the constant load test. Figure 9 illustrates the stress intensity factor history in this constant load-line displacement rate test. Similar to the constant load test (Figure 4), the stress intensity factor increased at a constant rate. However, in this test the

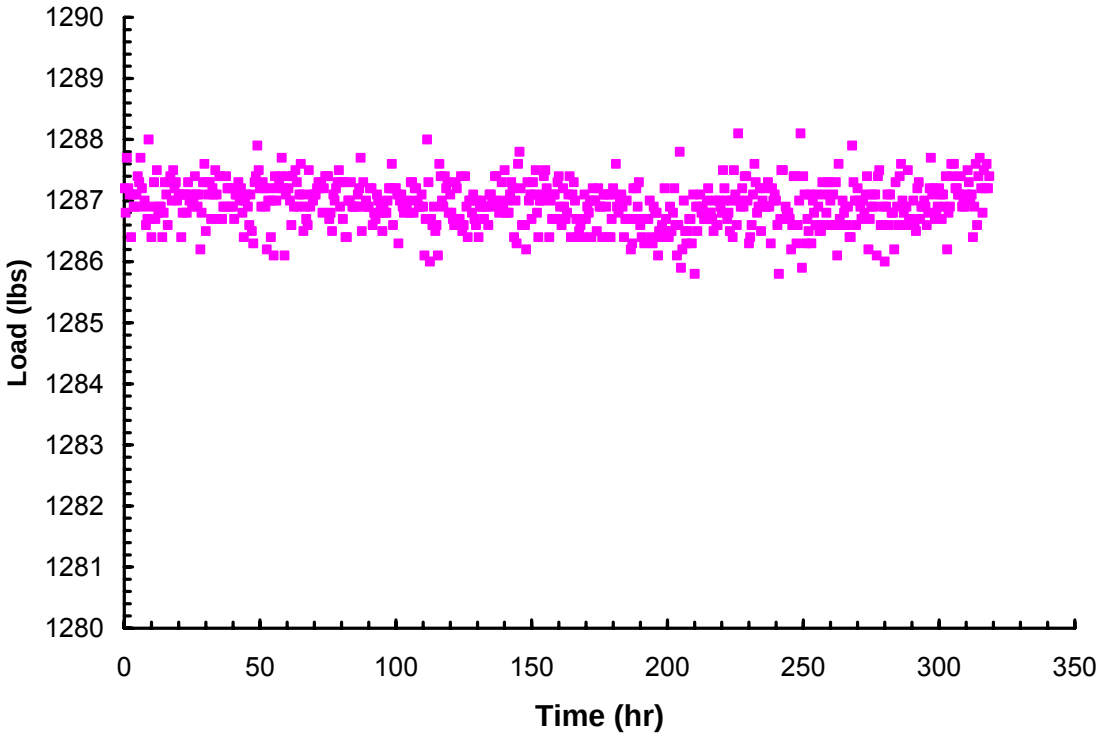

FIGURE 2: Load History in the X-750 AH Constant Load Test Conducted at 600°F (316°C) with 10 cc/kg Hydrogen at Stress Intensity Factor of 36.4 to 38.4 ksi√in (40.0 to 40.6 MPa√m)

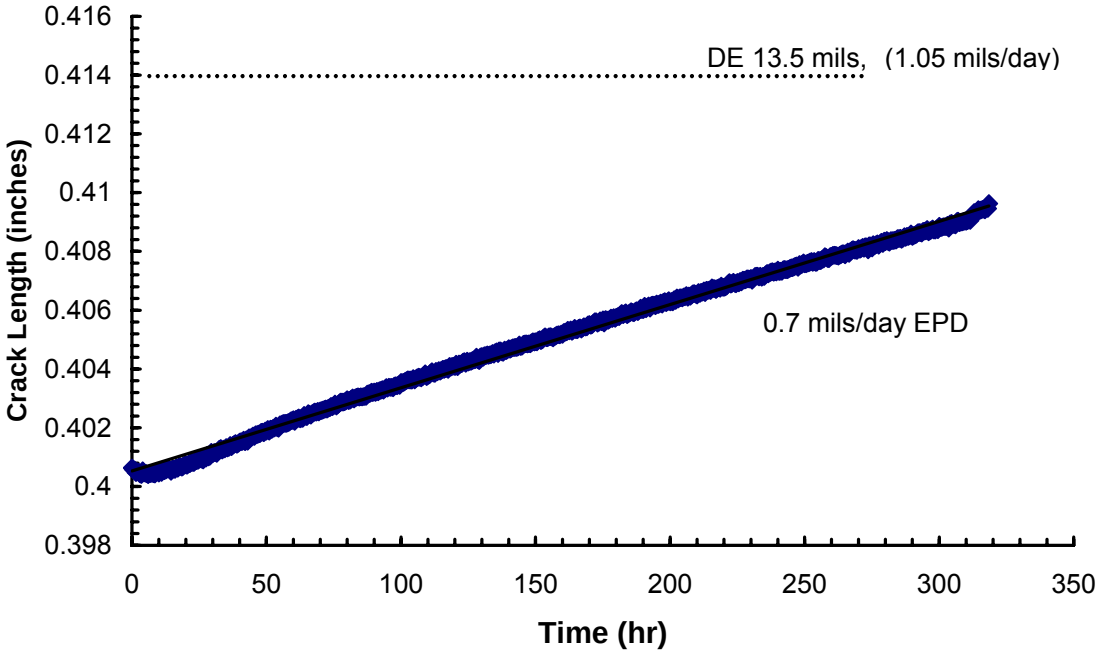

FIGURE 3: Comparison between EPD and DE Crack Measurements in the X-750 AH Constant Load Test Conducted at 600°F (316°C) with 10 cc/kg Hydrogen at Stress Intensity Factor of 36.4 to 38.4 ksi√in (40.0 to 40.6 MPa√m)

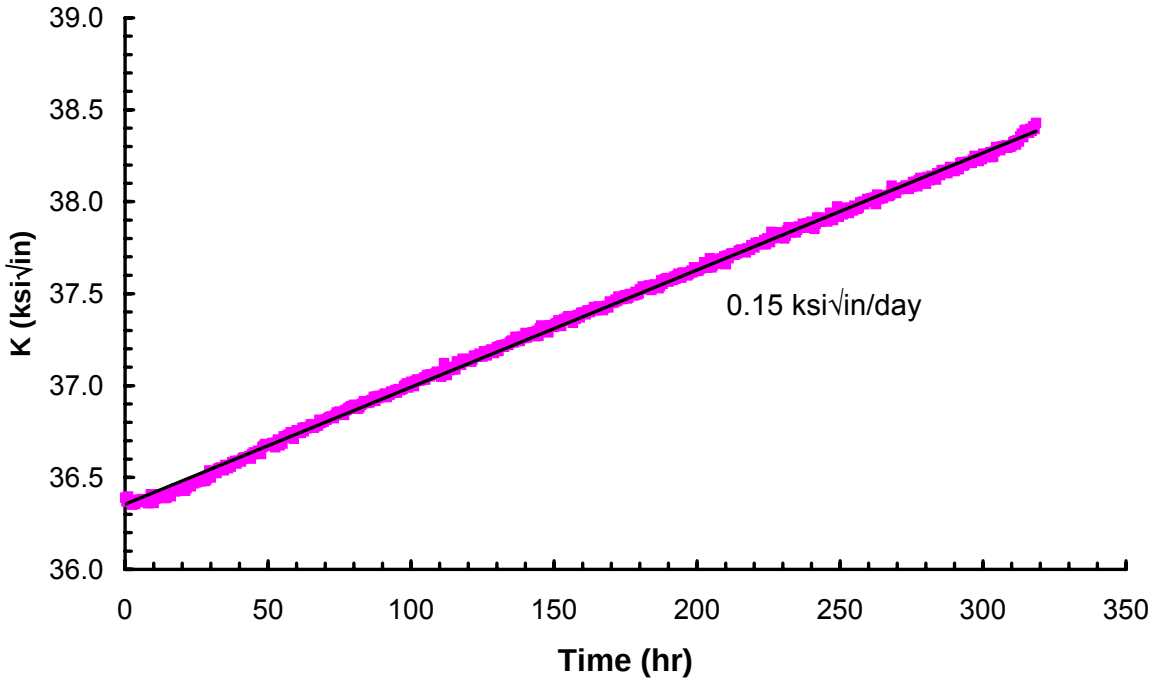

FIGURE 4: Stress Intensity Factor History in the X-750 AH Constant Load Test Conducted at 600°F (316°C) with 10 cc/kg Hydrogen at Stress Intensity Factor of 36.4 to 38.4 ksi√in (40.0 to 40.6 MPa√m)

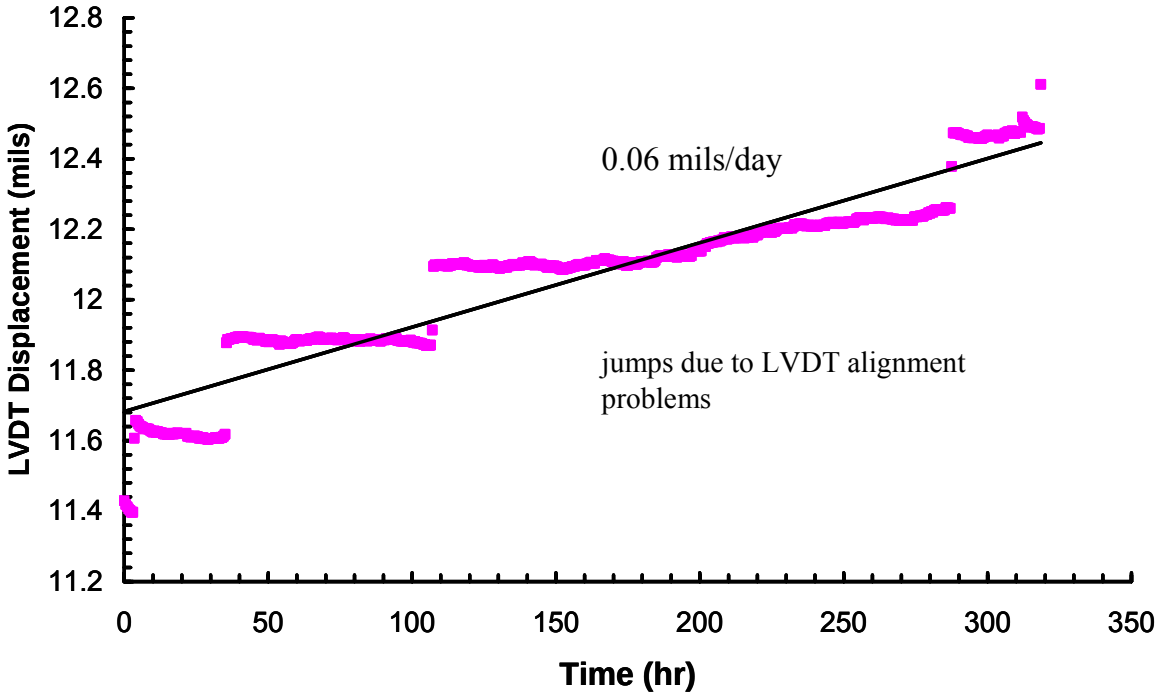

FIGURE 5: LVDT History in the X-750 AH Constant Load Test Conducted at 600°F (316°C) with 10 cc/kg Hydrogen at Stress Intensity Factor of 36.4 to 38.4 ksi√in (40.0 to 40.6 MPa√m)

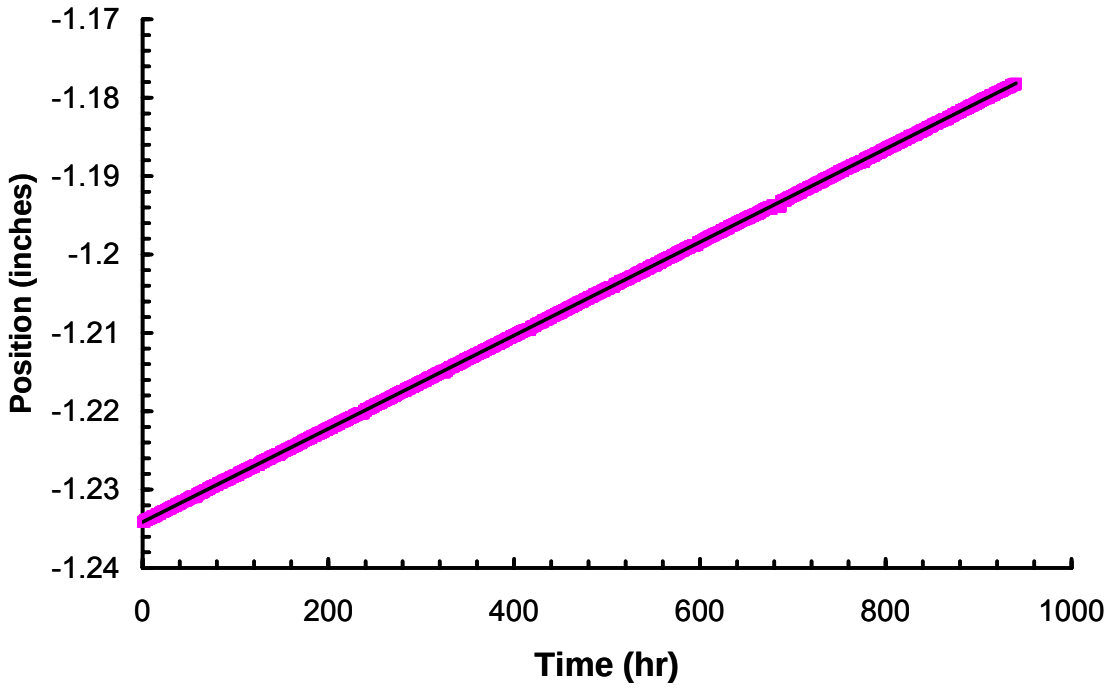

FIGURE 6: Actuator Position in the X-750 AH 0.00006 in/hr Constant Displacement Rate Test Conducted at 600°F with 10 cc/kg Hydrogen, Stress Intensity Factor of 10 to 68 ksi√in

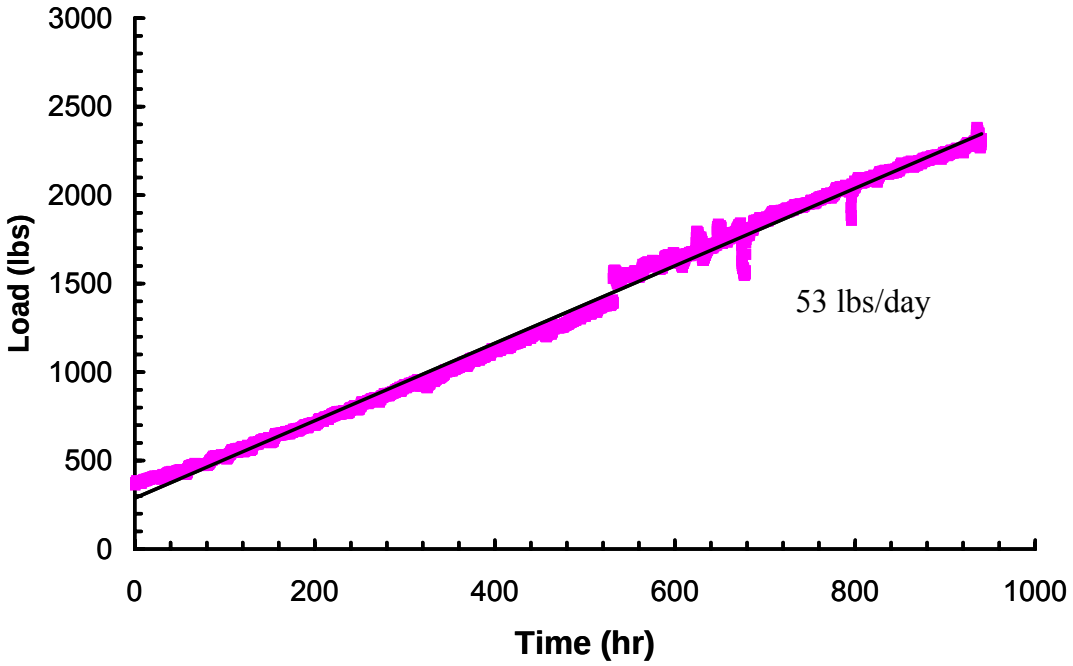

FIGURE 7: Load History in the X-750 AH 0.00006 in/hr Constant Displacement Rate Test Conducted at 600°F with 10 cc/kg Hydrogen, Stress Intensity Factor of 10 to 68 ksi√in

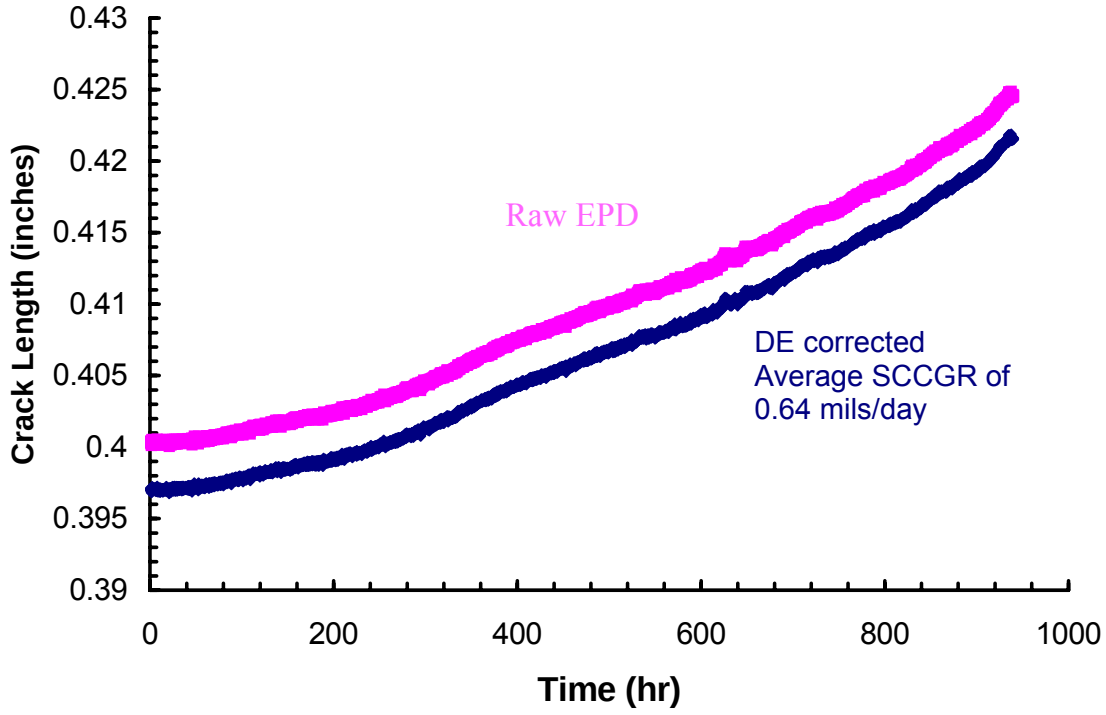

FIGURE 8: Crack Extension in the X-750 AH 0.00006 in/hr Constant Displacement Rate Test Conducted at 600°F with 10 cc/kg Hydrogen, Stress Intensity Factor of 10 to 68 ksi√in

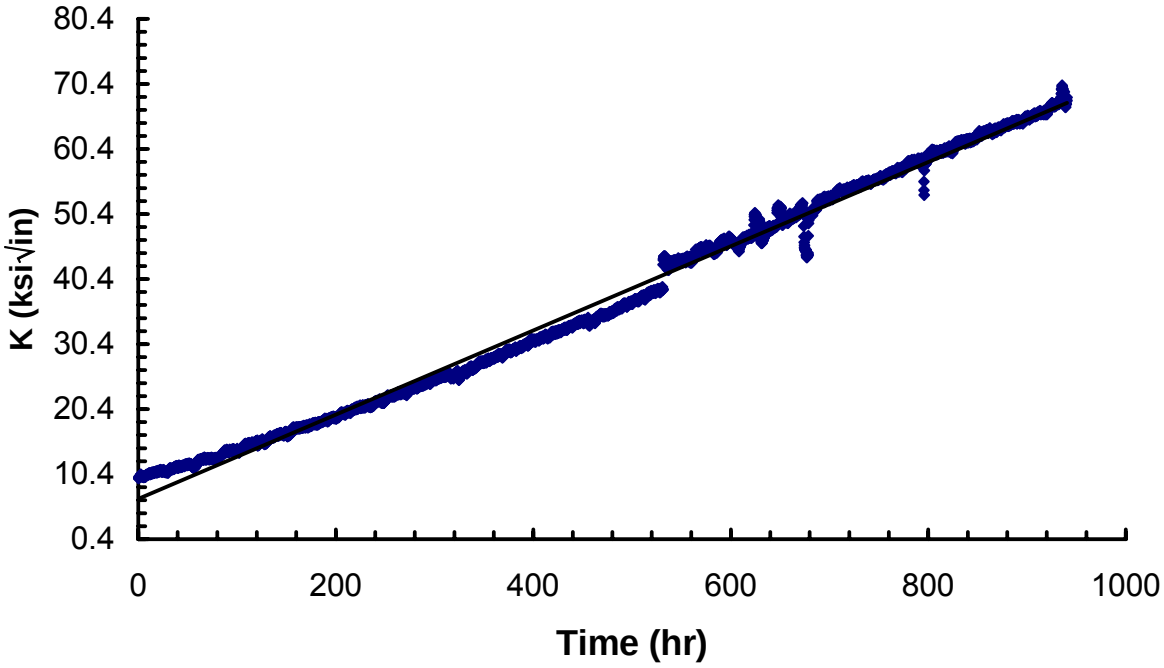

FIGURE 9: Stress Intensity Factor History in the X-750 AH 0.00006 in/hr Constant Displacement Rate Test Conducted at 600°F with 10 cc/kg Hydrogen

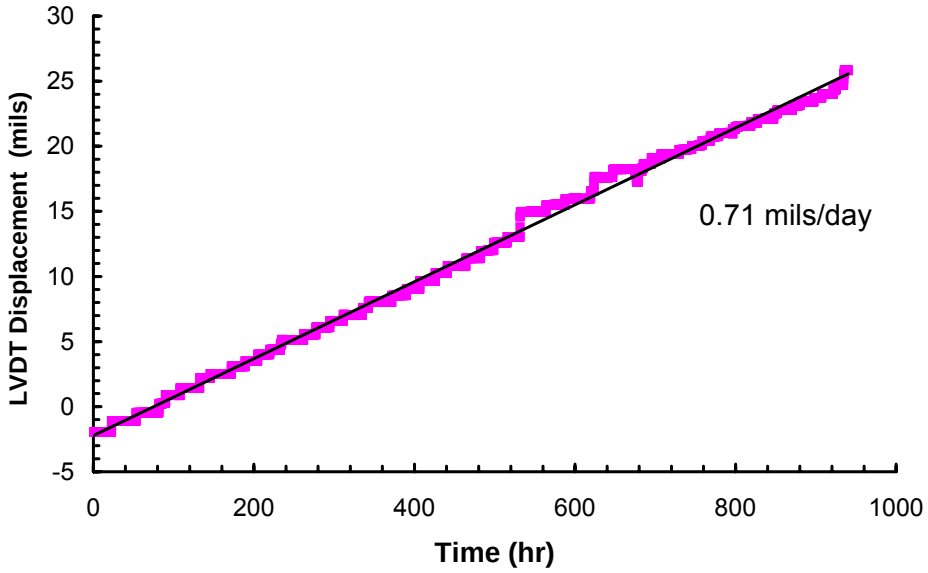

FIGURE 10: LVDT History in the X-750 AH 0.00006 in/hr Constant Displacement Rate Test Conducted at 600°F with 10 cc/kg Hydrogen

TABLE 2: X-750 AH TEST RESULTS: EFFECT OF LOAD-LINE DISPLACEMENT RATE

Specimen ID	EO6-04	HB1-02	HB1-01
Material	X-750	X-750	X-750
Heat	38F3X	38F3X	38F3X
Load Mode	Constant Load	Constant Position Rate	Constant Position Rate
Load (lbs)	1287	380 to 2300	400 to 2400
Displacement rate (in/hr)	NA	0.00006	0.0003
Total Time (days)	13.2	40.1	10.0
Incubation time (days)	0.4	1.67	1.25
B_{gross} (in)	0.398	0.398	0.398
B_{net} (in)	0.398	0.398	0.398
Width (in)	0.801	0.800	0.801
$a_{air\ fatigue\ precrack}$ (in)	0.411	0.397	0.407
$\Delta a_{SCC,ave}$ (mils)	13.5	24.6	8.7
$\Delta a_{SCC,max}$ (mils)	17.7	33.6	13.9
Ave SCCGR (mils/day)	1.05	0.64	0.99
K (ksi$\sqrt{in}$)[2]	36.4 to 38.4	10 to 68	11 to 69
LVDT measured load-line rate (mils/day)	0.06	0.71	3.6[3]
Load Rate (lbs/day)	NA	53	212
dK/dt (ksi$\sqrt{in}$/day)	0.15	1.6	6.1

[2] Stress intensity factor calculated according to ASTM E 399
[3] Estimated from the 0.00006 in/hr test LVDT measurement of 0.71 mils/day

rate (1.6 ksi√in/day (1.8 MPa√m/day)) was roughly 10 times faster. Additionally, in this test unlike the constant load test, the majority (90%) of the increase in the K level was due to the load increasing not due to the crack growth. The LVDT measured load-line displacement is provided in Figure 10. The load-line displacement rate was constant at 0.71 mils/day (18 μm/hr). And analogous to the rate of increase in the stress intensity factor, the load-line displacement rate was an order of magnitude faster in this load-line displacement rate test compared to the constant load test.

Constant Displacement Rate of 0.0003 in/hr (0.0076 mm/hr)

The test results from the 0.0003 in/hr (0.0076 mm/hr) displacement rate test are summarized in Figures 11 through 15 and in Table 2. In general, the trends and rates in this test were analogous to those in the 0.00006 in/hr test except that rates, apart from the SCCGR, were 4 to 5 times faster. Despite the greater displacement rate or change in the stress intensity factor (dK/dt), the DE corrected average SCCGR of 0.99 mils/day (1.05 μm/hr), Figure 13, was not appreciably different from the 0.64 mils/day (0.68 μm/hr) SCCGR observed in the 0.00006 in/hr displacement rate test or the 1.05 mils/day (1.11 μm/hr) observed in the constant load test.

An interesting observation noted in Figure 13 is that the uncorrected EPD crack extension over predicted the actual crack extension. EPD, typically, under predicts actual crack extension in constant load tests because of uncracked crack ligaments and non-uniformed crack fronts. These observations suggested that an EPD bias may be associated with load-line displacement or load rate testing. Crack opening, not extension, due to increasing load could be the source of an apparent EPD extension.

Figure 15 provides a representative SEM photograph of the fracture surface of the 0.0003 in/hr test specimen. This photograph illustrates that the cracking mode was completely intergranular (IG). Thus the load-line displacement rate test cracking mode was analogous to the cracking mode that occurs in constant load tests, namely IG SCC. Prior to these SEM inspection results there was concern that a different cracking mode (e.g., transgranular cracking, tearing) may occur in the load-line displacement rate tests. Such a difference would have been suggestive of a different cracking mechanism.

Discussion of Results

The relatively constant crack growth rates observed in both load-line displacement rate tests, despite the broad range of the stress intensity factor (~10-68 ksi√in), is consistent with the fact that the SCCGR K dependency of X-750 AH is very weak. In fact, Reference (9) reported that X-750 AH exhibits a classical two-stage crack velocity with rates being independent of K between 20 and 45 ksi√in.

Figure 16 provides a plot of the average test crack growth rate as a function of the load-line displacement rate and Figure 17 provides a plot of the average test crack growth rate as a function of rate of change in the stress intensity factor. These figures illustrate that for X-750 AH the SCC growth rate does not depend upon the load-line displacement rate. Specifically, the growth rate was the same (1 mil/day (1.1 μm/hr)) in the constant load and 0.0003 in/hr displacement rate tests even though the load-line displacement rate was >50 times faster in

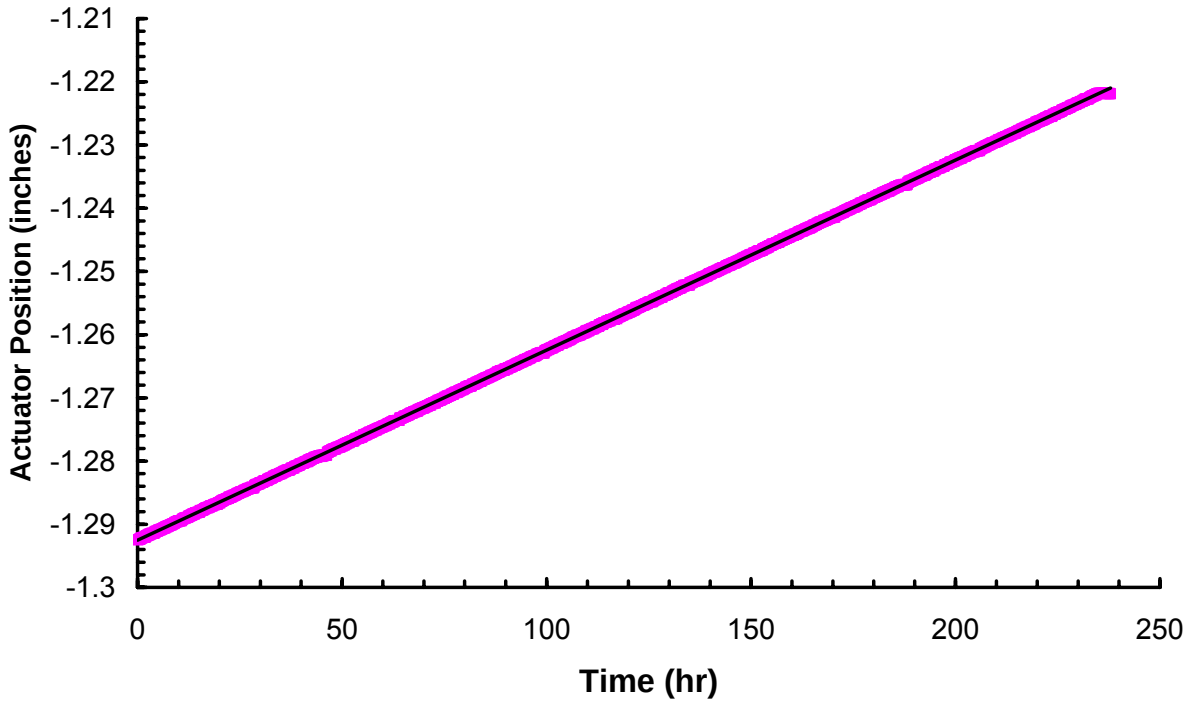

FIGURE 11: Actuator Position in the X-750 AH 0.0003 in/hr Constant Displacement Rate Test Conducted at 600°F with 10 cc/kg Hydrogen, Stress Intensity Factor of 11 to 69 ksi√in

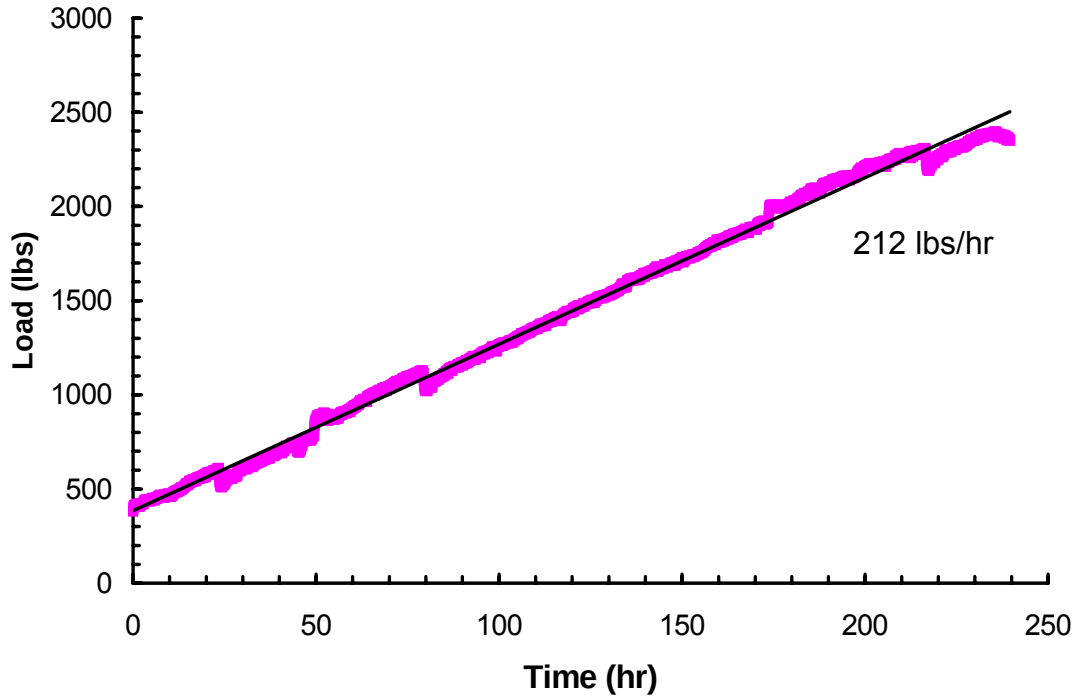

FIGURE 12: Load History in the X-750 AH 0.0003 in/hr Constant Displacement Rate Test Conducted at 600°F with 10 cc/kg Hydrogen, Stress Intensity Factor of 11 to 69 ksi√in

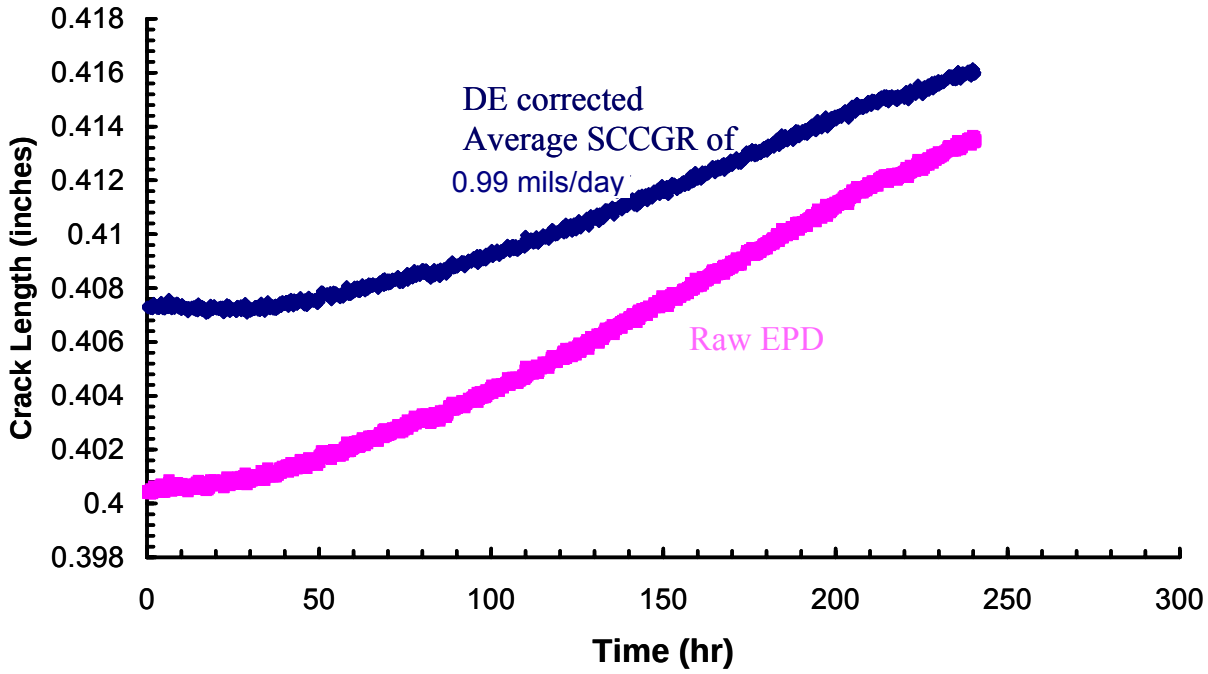

FIGURE 13: Crack Extension in the X-750 AH 0.0003 in/hr Constant Displacement Rate Test Conducted at 600°F with 10 cc/kg Hydrogen, Stress Intensity Factor of 11 to 69 ksi√in

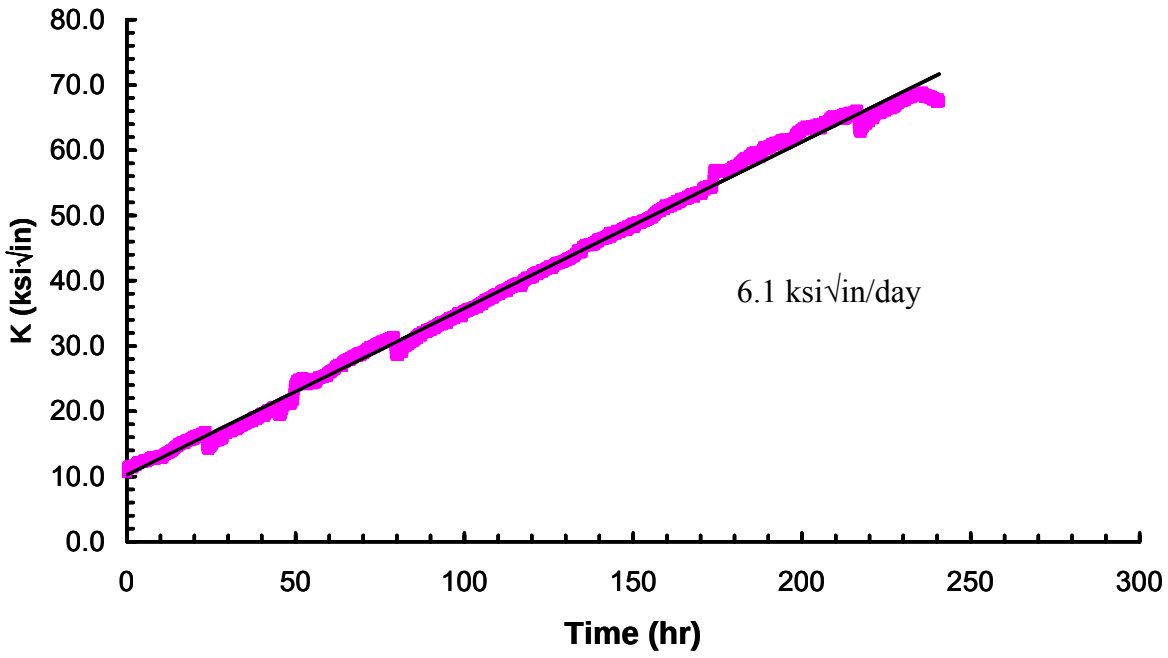

FIGURE 14: Stress Intensity Factor History in the X-750 AH 0.0003 in/hr Constant Displacement Rate Test Conducted at 600°F with 10 cc/kg Hydrogen

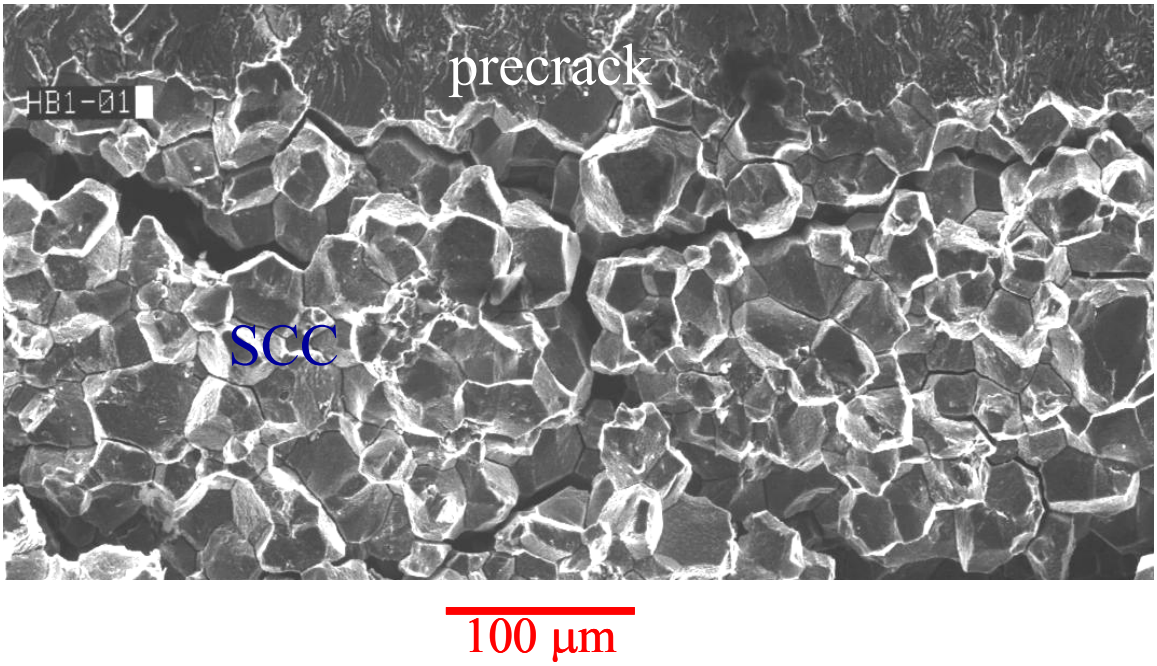

FIGURE 15: SEM Fracture Surface Inspection of the X-750 AH 0.0003 in/hr Constant Displacement Rate Test Specimen Revealing Intergranular SCC

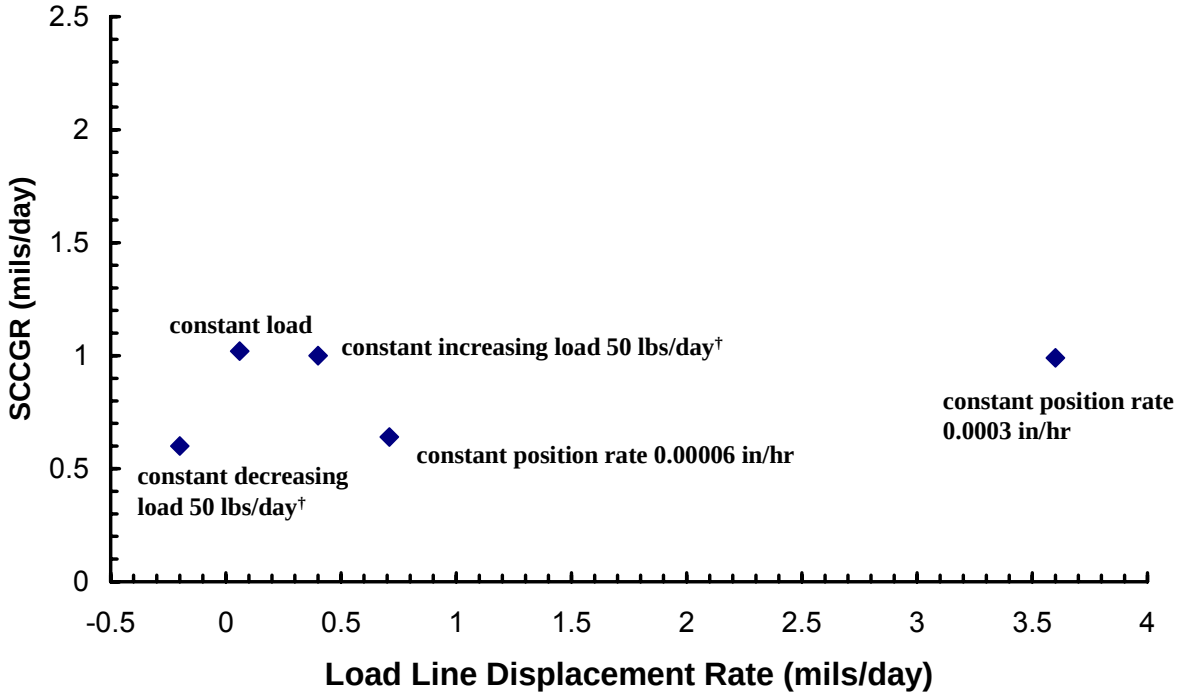

† SCCGRs were estimated through DE corrected EPD

FIGURE 16: X-750 AH SCC Growth Rate as a Function of the Specimen Load-Line Displacement Rate. Results Indicate that X-750 AH SCCGR is not Appreciably Dependent Upon the Loading Rate (i.e., deformation rate)

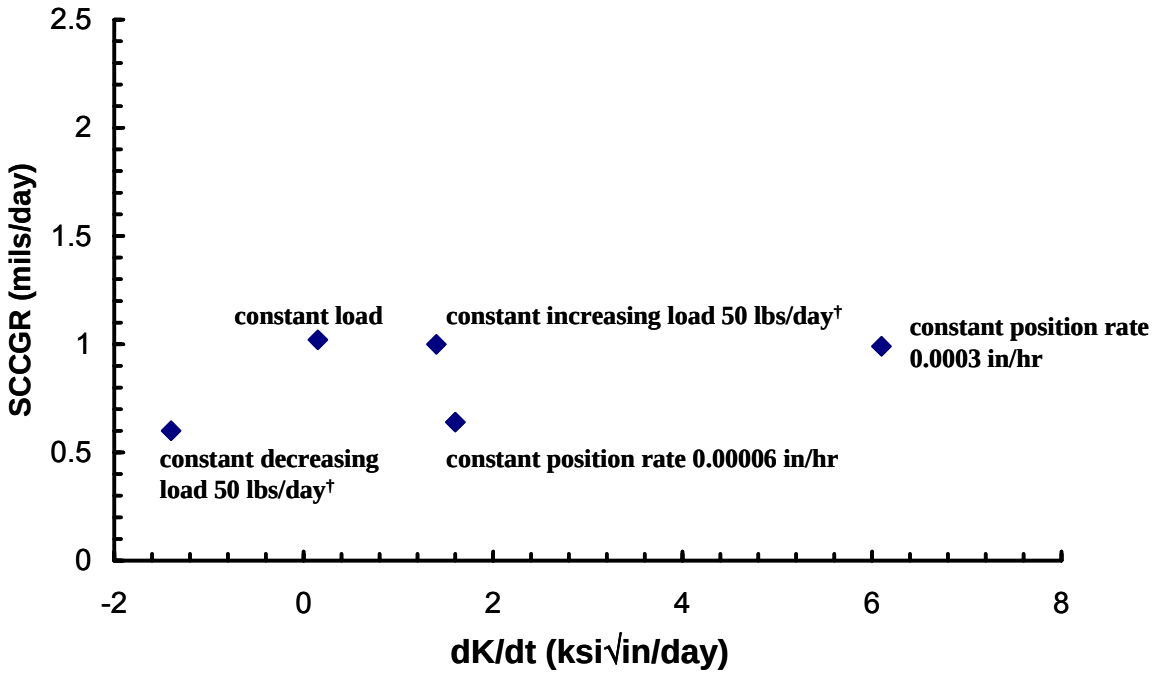

† SCCGRs were estimated through DE corrected EPD

FIGURE 17: X-750 AH SCC Growth Rate as a Function of the Rate of Increase in K. Results Indicate that X-750 AH SCCGR is not Appreciably Dependent Upon the Loading Rate (i.e., deformation/creep rate)

the 0.0003 in/hr load-line displacement rate test. Since the deformation/creep rate within the crack tip plastic zone is proportional to the test load-line displacement rate, these results indicate that the mechanism of X-750 AH SCC growth does not depend highly on the deformation/creep rate. These results indicate that deformation or creep based models (e.g., HACF, FRO) are fundamentally inappropriate for X-750 AH crack growth.

$$\dot{a}_{\text{X-750AH}} \not\propto \dot{\varepsilon}_{ct} \propto \underset{rate}{Displacement}$$

Strictly speaking, these results are only applicable to X-750 AH. However, because of the similarities between the SCC response of X-750, Alloy 600 and EN82H, it is likely that the same SCC rate controlling step occurs for all these alloys. For example, X-750 AH has nearly the same thermal activation energy (Q) as Alloy 600 and EN82H[10]. Also X-750 AH, X-750 HTH, Alloy 600 and EN82H all show similar coolant hydrogen dependencies[10], see Figure 18. These X-750 AH results therefore suggest that deformation based models are also inappropriate for Alloy 600 and its weld metal EN82H.

Data from the three tests (i.e., constant load test and two load-line displacement rate tests) which were discussed in the prior sections is included in Figures 16 and 17. Two additional data points are also included in these figures. These data points are labeled as “constant

decreasing load 50 lbs/day" and "constant increasing load 50 lbs/day". These two SCCGRs were obtained from a single X-750 AH compact tension specimen that was tested at both a

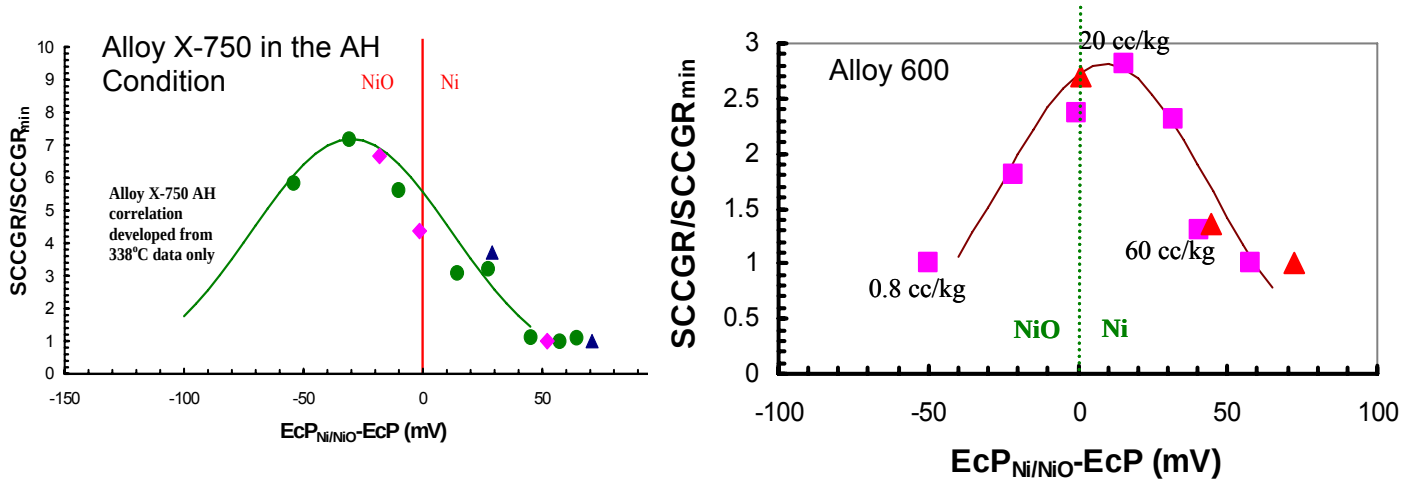

FIGURE 18: Comparsion between Alloy 600 and X-750 AH Coolant Hydrogen SCC Functionalities[10].

constant increasing loading rate of 50 lbs/day and a constant decreasing loading rate of 50 lbs/day. Because of the multiple test conditions associated with this specimen these two SCCGRs were determined through DE corrected EPD. The uncertainty in an EPD determined SCCGR is greater than the uncertainty of a DE determined SCCGR. The observed SCCGRs at these two conditions are, however, consistent with the observations from the single test condition specimens; that is, X-750 AH SCC growth rate is independent of the load-line displacement rate.

Figure 19 compares the crack growth rates measured in this study as a function of the stress intensity. Experimentally, little or no K dependency was noted. The weak stress intensity factor and load-line displacement dependency of X-750, Figures 16,17,19, and the significant coolant H_2 and temperature dependency of this alloy strongly suggests that the rate controlling step for X-750 crack growth is corrosion or environmentally controlled. Figure 20, for example, compares observed SCC growth rate data at 600°F as a function of coolant H_2, Reference (10), to the load-line displacement data generated in this study at 600°F. The same heat of X-750 AH was employed in both studies. This figure illustrates an appreciable coolant hydrogen effect ~7X and an experimentally insignificant load-line displacement effect.

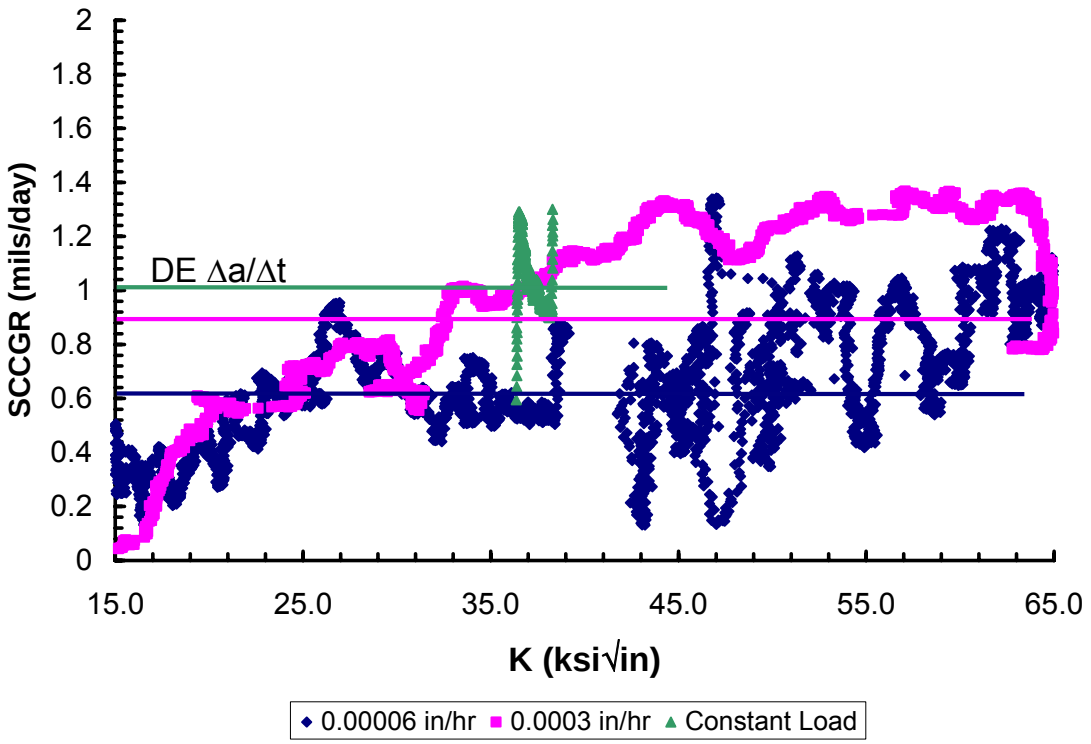

FIGURE 19: Comparison between EPD and DE SCCGRs at 600°F as a Function of the Stress Intensity Factor

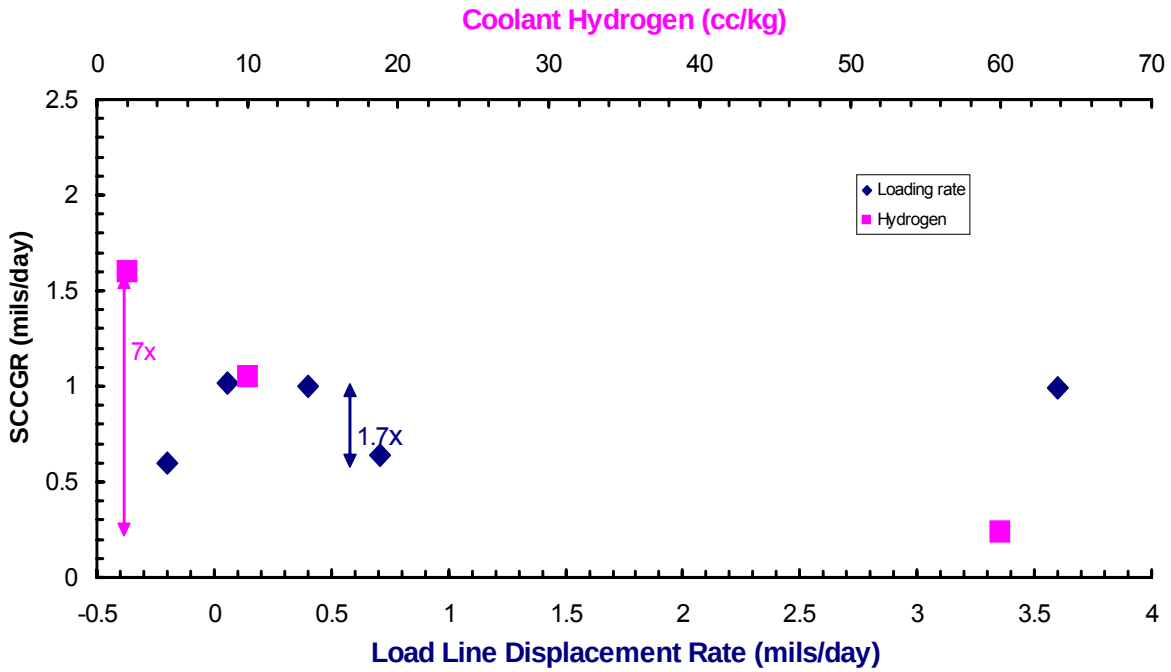

FIGURE 20: Figure Comparing the Role of the Environmental Parameter (Hydrogen Concentration) with the Mechanical Parameter (Load Line Displacement Rate)

CONCLUSIONS

- X-750 AH SCC growth rate is not dependent upon the load-line displacement rate. In this study, load-line displacement rate tests with load-line displacement rates >50x faster than load-line displacement rates in conventional constant load tests did not alter the SCC growth rate. The load-line displacement rate is proportional to the deformation/creep rate within the crack tip plastic zone. These results, therefore, indicate that the mechanism of X-750 AH SCC growth does not depend highly on the deformation/creep rate.

- It is likely that X-750 AH crack growth rate is controlled by an environmental or corrosion driven process because of the weak mechanical (e.g., K and load-line displacement) and strong environmental (temperature and coolant H_2) dependencies which are associated with this alloy. Additionally, the similarities between the SCC response of X-750, Alloy 600 and EN82H (e.g., similar temperature and coolant hydrogen response) suggests that it is likely that the same SCC process is occurring for all these alloys (i.e., the same rate controlling step) and that deformation based models are also inappropriate for Alloy 600 and EN82H.

- The in-situ electrical potential drop (EPD) crack monitor over predicted the actual crack extension in load-line displacement rate tests. This over prediction is in contrast to the under prediction that occurs in constant load testing suggesting a possible EPD bias due to load-line displacement/load increases.

REFERENCES

1. TM Angeliu, PL Andresen and FP Ford, “Applying Slip-Oxidation to the SCC of Austenitic Materials in BWR/PWR Environments”, CORROSION/98. Paper no. 98262. (Houston, TX:NACE 1998)

2. MM Hall and DM Symons, “Hydrogen Assisted Creep Fracture Model for Low Potential Stress Corrosion Cracking of Ni-Cr-Fe Alloys”, *Chemistry and Electrochemistry of Corrosion and Stress Corrosion Cracking: A Symposium Honoring the Contributions of RW Staehle*, The Material Society, New Orleans, LA, (February 2001). p. 447

3. GA White, “Development of Crack Growth Rate Disposition Curves for Primary Water Stress Corrosion Cracking (PWSCC) of Alloy 82, 182 and 132 Weldments”, 12th International Symposium in Environmental Degradation of Materials in Nuclear Power Systems-Water Reactors, (Salt Lake City, UT: TMS 2005)

4. JS Fish, N Lewis, WJS Yang, DJ Perry and CD Thompson, “AEM Investigations of Primary Water SCC in Nickel Alloys”, 8th International Symposium on Environmental Degradation of Materials in Nuclear Power Systems-Water Reactors, (Amelia Island, FL:ANS 1997), p.266

5. DS Morton, D Gladding, MK Schurman and CD Thompson, “Effect of Soluble Zinc Addition on the SCC Performance of Nickel Alloys in Deaerated Hydrogenated Water”, 8th International Symposium on Environmental Degradation of Materials in Nuclear Power Systems-Water Reactors, (Amelia Island, FL:ANS 1997), p.387

6. SE Ziemniak, ME Jones, and KES Combs, Journal of Solution Chemistry, (1995), Vol. 24, p. 837

7. CD Thompson, DM Carey and NL Perazzo, “Effects of Hydrogen on Electropotential Monitoring of Stress Corrosion Crack Growth”, 8th International Symposium on Environmental Degradation of Materials in Nuclear Power Systems-Water Reactors, (Amelia Island, FL:ANS 1997), p.366

8. SA Attanasio, DS Morton, and MA Ando, “Measurement and Calculation of Electrochemical Potentials in Hydrogenated High Temperature Water, including an Evaluation of the Yttria-Stabilized Zirconia/Iron-Iron Oxide (Fe/Fe_3O_4) Probe as a Reference Electrode”, CORROSION/02. Paper no. 02517. (NACE 2002)

9. WJ Mills, MR Lebo, and JJ Kearns, “Hydrogen Embrittlement, Grain Boundary Segregation and Stress Corrosion Cracking of X-750 in Low and High-Temperature Water”, Metallurgical and Materials Transactions, (June 1999), p. 1579

10. DS Morton, SA Attanasio, E Richey and GA Young, “In Search of the True Temperature and Stress Intensity Factor Dependencies For PWSCC”, 12th International Symposium on Environmental Degradation of Materials in Nuclear Power Systems-Water Reactors, (Salt Lake City, UT: TMS 2005)